

MASTER

FAILURE ANALYSIS OF GLASS-CERAMIC INSULATORS OF SHOCK TESTED VACUUM (NEUTRON) TUBES

R. K. Spears
Metallurgy and Ceramics Laboratory

August 25, 1980

General Electric Company
Neutron Devices Department
P. O. Box 11508
St. Petersburg, Florida 33733

Prepared for the
U. S. Department of Energy
Albuquerque Operations Office
Under Contract No. DE-AC04-76DP00656

DISCLAIMER

This book was prepared as an account of work sponsored by an agency of the United States Government. Neither the United States Government nor any agency thereof, nor any of their employees, makes any warranty, express or implied, or assumes any legal liability or responsibility for the accuracy, completeness, or usefulness of any information, apparatus, product, or process disclosed, or represents that its use would not infringe privately owned rights. Reference herein to any specific commercial product, process, or service by trade name, trademark, manufacturer, or otherwise, does not necessarily constitute or imply its endorsement, recommendation, or favoring by the United States Government or any agency thereof. The views and opinions of authors expressed herein do not necessarily state or reflect those of the United States Government or any agency thereof.

DISTRIBUTION OF THIS DOCUMENT IS UNLIMITED

Rey

DISCLAIMER

This report was prepared as an account of work sponsored by an agency of the United States Government. Neither the United States Government nor any agency thereof, nor any of their employees, makes any warranty, express or implied, or assumes any legal liability or responsibility for the accuracy, completeness, or usefulness of any information, apparatus, product, or process disclosed, or represents that its use would not infringe privately owned rights. Reference herein to any specific commercial product, process, or service by trade name, trademark, manufacturer, or otherwise does not necessarily constitute or imply its endorsement, recommendation, or favoring by the United States Government or any agency thereof. The views and opinions of authors expressed herein do not necessarily state or reflect those of the United States Government or any agency thereof.

DISCLAIMER

Portions of this document may be illegible in electronic image products. Images are produced from the best available original document.

NOTICE

This report was prepared as an account of work sponsored by the United States Government. Neither the United States nor the United States Department of Energy, nor any of their employees, nor any of their contractors, subcontractors, or their employees, makes any warranty, express or implied, or assumes any legal liability or responsibility for the accuracy, completeness or usefulness of any information, apparatus, product or process disclosed, or represents that its use would not infringe privately-owned rights.

Printed in the United States of America
Available from
National Technical Information Service
U.S. Department of Commerce
5285 Port Royal Road
Springfield, VA 22161
Price: Printed Copy \$ 4.50 ;Microfiche \$2.25

ABSTRACT

Eight investigative techniques were used to examine the glass-ceramic insulators in vacuum (neutron) tubes. The insulators were extracted from units that had been subjected to low temperature mechanical shock tests. Two of the three units showed reduced neutron output after these tests and an insulator on one of these two was cracked completely through which probably occurred during shock testing. The objective of this study was to determine if any major differences existed between the insulators of these tubes. After eight analyses, it was concluded that no appreciable differences existed. It appeared that cracking of the one glass-ceramic sample was initiated at inner-sleeve interface voids. For this sample, the interface void density was much higher than is presently acceptable. All insulators were made with glass-ceramic having an Na_2O content of 4.6 wt%. An increased Na_2O content will cause an increase in the coefficient of expansion and will reduce the residual stress level since the molybdenum has a higher coefficient of thermal expansion than the insulator. Thus, it is believed that a decrease in interface voids and an increase in Na_2O should aid in reduced cracking of the insulator during these tests.

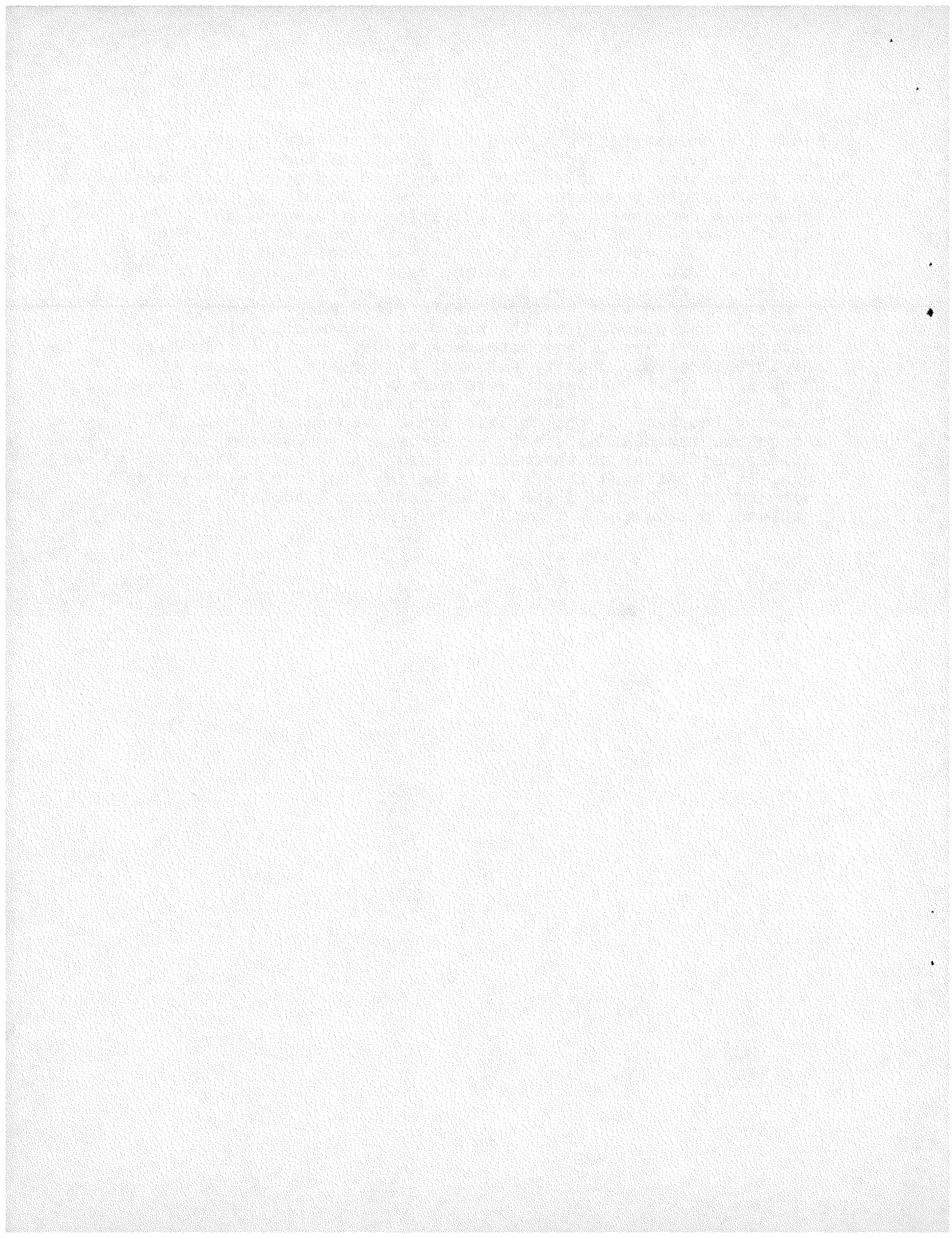


TABLE OF CONTENTS

Section	Page
INTRODUCTION	1
EXPERIMENTAL APPROACH	2
PROCEDURES AND RESULTS	3
Delamination of Molybdenum	3
Fractographic Examination of Insulators	4
Insulator A	4
Insulator B	4
Insulator C	10
Interface Void Analysis	10
Percent Sodium	13
Chemical Element Comparison by X-ray Emission Spectroscopy	19
Coefficient of Expansion	19
Differential Thermal Analysis	20
Microstructure	20
RESULTS	20
ACKNOWLEDGMENTS	21
REFERENCES	21
DISTRIBUTION	23

TABLE

Number	Page
1 Glass-Ceramic Composition Specification	2

ILLUSTRATIONS

Number	Page
1 Vacuum Tube Envelope	1
2 Bottom View of Insulator A	5
3 Photograph and Schematic, Crack C1, Insulator A	6

ILLUSTRATIONS

Number		Page
4	Photograph and Schematic, Crack C2, Insulator A	7
5	Photograph and Schematic, Bottom View, Insulator B	8
6	Photograph of Crack No. 1. Insulator B	9
7	Photograph of Crack No. 2. Insulator B	9
8	Photograph of Bottom Surface, Insulator C	10
9	Photograph and Schematic, Bottom View, Insulator C	11
10	Photograph and Schematic, Fracture in Insulator C	12
11	SEM Photograph, Insulator-Sleeve Interface. Insulator A. 100X Magnification	14
12	SEM Photograph, Insulator-Sleeve Interface. Insulator A. 1000X Magnification	14
13	SEM Photograph, Insulator Sleeve Interface. Insulator B. 60X Magnification	15
14	SEM Photographs, Insulator-Sleeve Interface. Insulator B. 300X Magnification	15
15	SEM Photograph Showing Large Scratch and Smaller Polishing Scratches. Insulator B	16
16	SEM Photograph Showing Scratch and Voids Lodged in Scratches. Insulator B	16
17	SEM Photograph Showing Scratches. Insulator A	17
18	SEM Photograph Showing Cluster of Voids. Insulator A	17
19	SEM Photograph, Magnified View of Cluster Shown in Figure 18. Insulator A	18
20	Graphical Comparison of Chemical Differences Detected in Insulators Using X-ray Emission	19
21	Comparison of Differential Thermal Analysis Thermograms. Insulator A	21

INTRODUCTION

A loss in neutron output occurred on several neutron tubes that had been subjected to low-temperature mechanical shock tests at the General Electric Neutron Devices Department (GEND). The encapsulated assembly consists of a vacuum (neutron) tube and an electronic power supply. The vacuum tube envelope consists of an inner sleeve, an insulator and an outer frame (Figure 1). The low-temperature mechanical shock environmental tests consisted of subjecting the unit to a 3500 g level in each direction parallel to the axis of the tube, at a 3500 g level in a direction normal to the tube axis and at a 2000 g level normal to the tube axis but 90° from the 3500 g normal direction. The temperature during these tests was -55°C and testing was performed on a sled with an impact duration of 0.001 seconds.

46HA922318-1

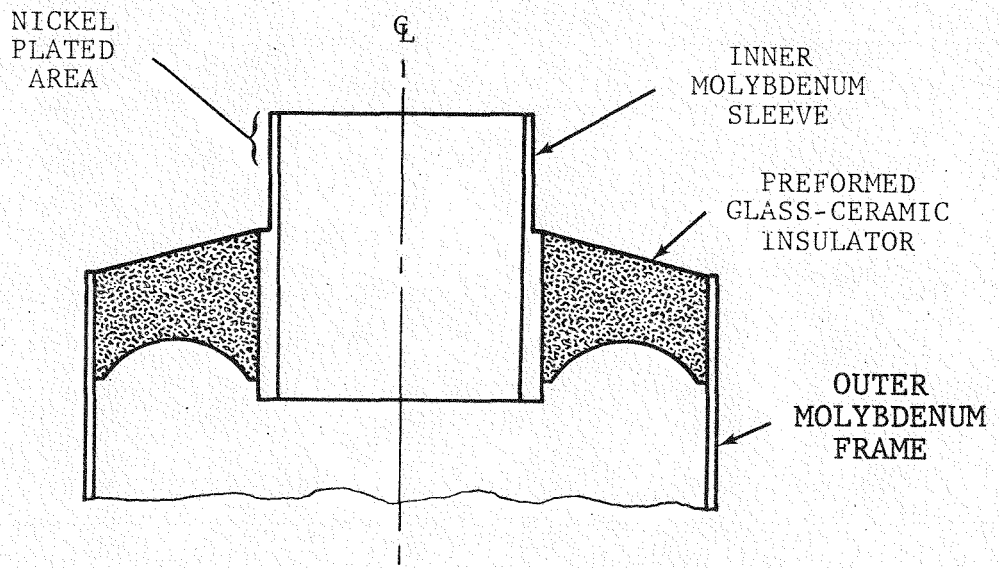


Figure 1. Vacuum Tube Envelope

Three units were submitted for analysis. Of those, one was a control sample (designated as unit C for this study) that showed no reduction in neutron output after environmental tests. Both of the other two units (designated as units A and B) showed a 30 percent reduction in output. A Zyglo* examination for cracking of the insulator showed that one of the tubes was grossly cracked and the crack extended through

*Trademark, Magnaflux Corp.

the glass-ceramic. The second tube showed adsorption only at the edge of the insulator frame (the Zyglo examination was made on the inside of the tube only) and the crack paths were not continuous to the outer surface of the tube insulator. The tubes of both low output units showed Zyglo adsorption at a target end brazement. Several undesirable problems were present in this region.¹

Since the glass-ceramic insulator of the tube is a suspect region for loss of vacuum integrity, the insulators of these three tubes were submitted to the GEND Metallurgy and Ceramics Laboratory for analysis. The purpose of this analysis was to determine the integrity of the glass-ceramic insulators, to determine any differences between the three insulators and to determine the adequacy of the insulator-molybdenum seal. The composition specification of the glass-ceramic is shown in Table 1.

Table 1. Glass-Ceramic Composition Specification

Compound	Weight Percent
Al ₂ O ₃	9.5
BaO	4.8
Na ₂ O	4.6
P ₂ O ₅	2.5
SiO ₂	46.4
ZnO	32.2

EXPERIMENTAL APPROACH

The plan outlining the tests recommended that eight examinations be performed on the insulators. The test samples submitted consisted of the half of the tube containing the insulator.

One of the test methods used was fractography, the microscopic examination of fractured surfaces. In general, fracture in glass is characterized by the following features that emanate from the crack origin: (1) the mirror region (characterized by a smooth, flat area), (2) the mist region (characterized by an area that is grainy or misty in appearance), (3) hackle (characterized by ridges which run in the direction of fracture propagation, with individual ridges resembling the veins of a feather) and (4) rib marks (a rib mark consists of a sharp change in the direction of the crack). Other features sometimes present are smooth wave-like patterns called Wallner lines that lie in the mirror region and usually terminate in the mist region. Wallner lines are useful in determining the shape of the fracture propagation front as well as the speed and direction of propagation of the crack.

A comprehensive analysis of fractures in brittle materials usually includes scanning electron microscope and/or transmission electron microscope examinations. However, in most cases the important information to be attained is the crack origin, direction of principal stress (normal to the mirror region at the crack source) and crack propagation direction. An unaided or low magnification examination is usually adequate to attain this information. Of primary interest is the origin of the crack. Fractographic analysis will also indicate the manner in which the mechanical stress causing failure was applied.

PROCEDURES AND RESULTS

DELAMINATION OF MOLYBDENUM

The molybdenum frame below the insulator was cut from the part submitted. This was etched for five to ten seconds in the etchant to remove any smeared metal at the cut end. The part was then Zyglo impregnated and the top and bottom edges were examined under ultraviolet light on a stereomicroscope.

Delamination was not observed on any of the molybdenum rings examined. All frames showed areas in which the Zyglo had adsorbed into the grain boundaries. This may have resulted from the etchant used to remove the smeared metal in that the etchant may have attacked the grain boundary allowing it to adsorb Zyglo.

FRACTOGRAPHIC EXAMINATION OF INSULATORS

When the insulators were examined it was found that all insulators were cracked. Thus, it is concluded that the control tube insulator became cracked during its removal from the unit. The molybdenum was etched from the insulator and each individual glass piece of the insulator was examined to determine the origin of the crack. A stereomicroscope, rather than SEM or TEM, was used for this examination.

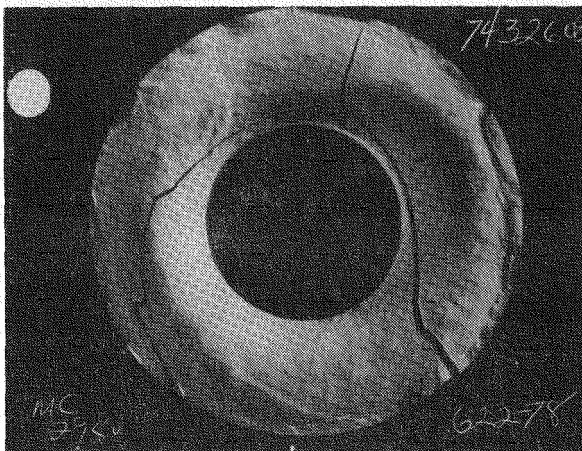
Insulator A

The bottom view of this insulator (looking from the inside of the tube out) with the molybdenum removed is shown in Figure 2-A. A crack shown by dotted lines of Figure 2-B was present in the insulator but separation did not occur until manually forced. Five pieces (as noted in Figure 2-B) were available for visual examination. Crack origins were observed at two locations (C1 and C2, Figure 2-B) near the top surface of the insulator.

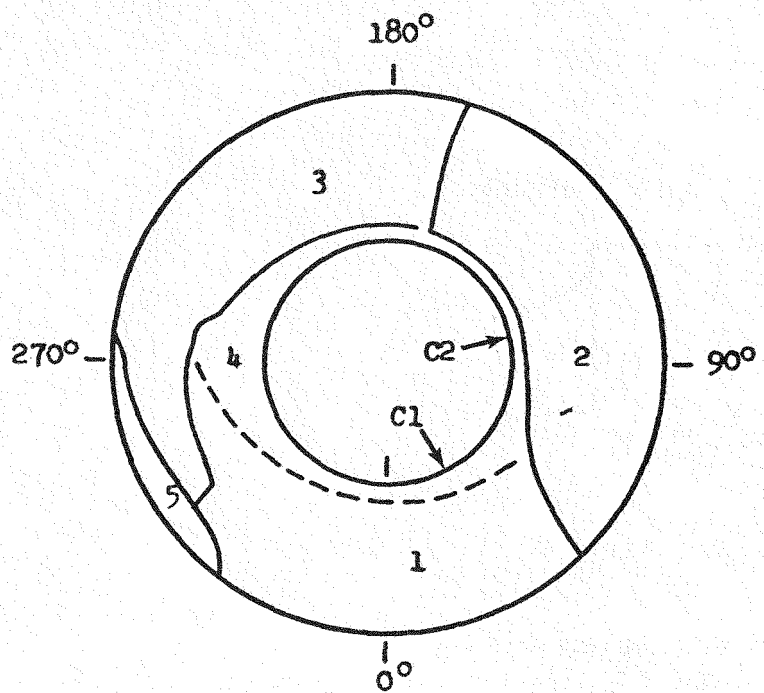
Figure 3 shows views of crack C1. This crack occurred very near the inner sleeve and originated at a cluster of interface voids of 0.005 to 0.015 in. diameter. The second crack originated approximately 80 to 90° from the first (see Figure 4). Voids were also evident at the point of initiation. This crack was more typical of fracture patterns observed in brittle materials in that a mirror region, a mist region (with Wallner lines) and hackel was clearly evident. The glass adhered adequately to the molybdenum and only in the region where the crack initiated was unbonding evident.

Insulator B

The bottom view of this insulator, after the cracked portions were manually separated, is shown in Figure 5. Five pieces (marked in Figure 5-B) were available for investigation. As with the previous insulator, two cracks were evident, one at 5° and the other at 80°. These cracks originated close to the inner sleeve but near the bottom surface of the tube rather than the top surface as was observed on Insulator A. Voids at the point of crack origin were not apparent in either crack. A photograph of crack no. 1 at 5° from the origin is shown in Figure 6. Figure 7 is a similar photograph of crack no. 2 at 80° from the origin.

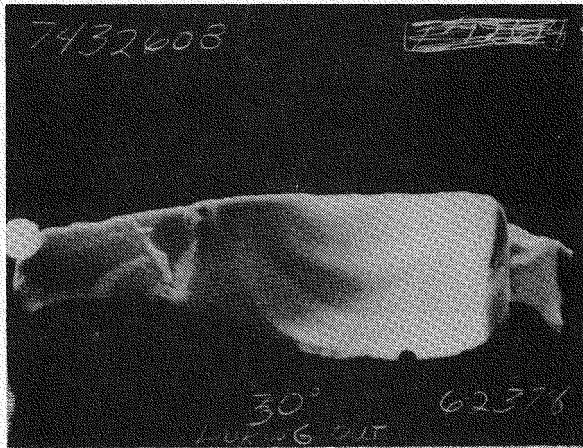


A. Photograph. (The molybdenum has been etched away.)

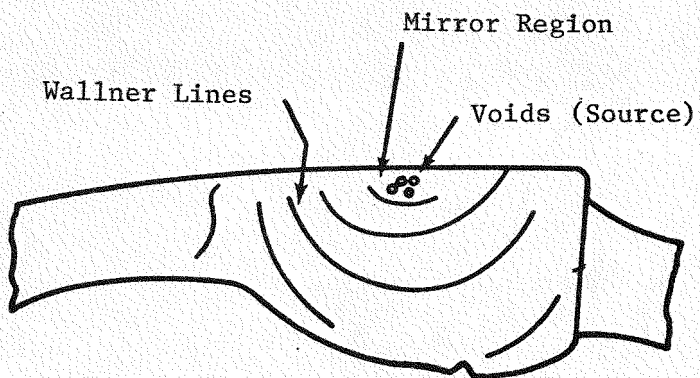


B. Schematic. (The cracks originated at C1 and C2 near the top surface.)

Figure 2. Bottom View of Insulator A
(Looking From Inside of Tube)

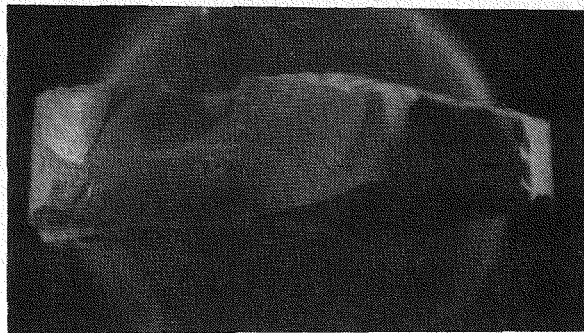


A. Photograph Showing Voids at Origin. (Wallner lines are also evident.)

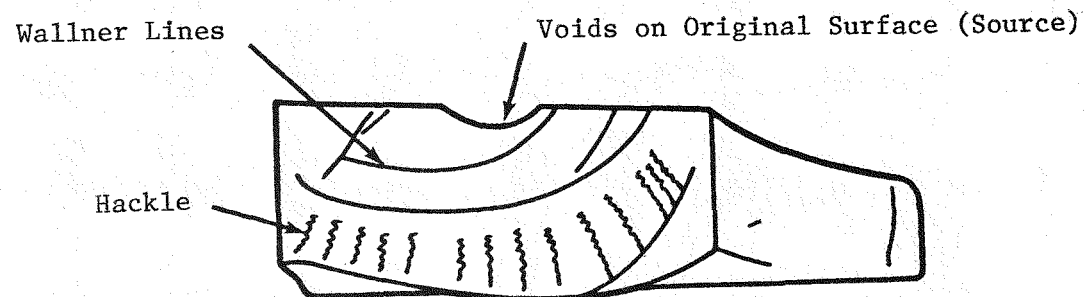


B. Schematic of Fracture Area

Figure 3. Photograph and Schematic, Crack C1, Insulator A

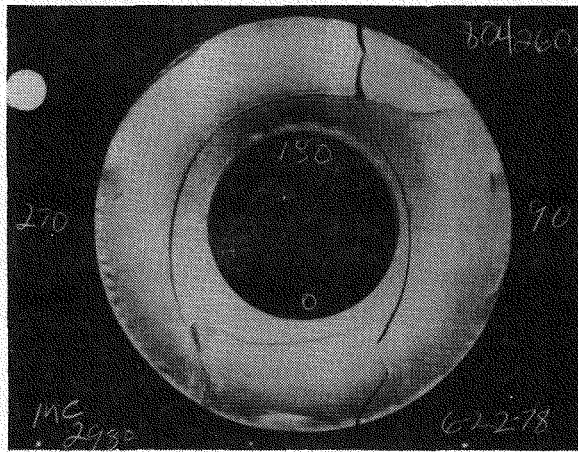


A. Photograph. (Void area has been broken off. Wallner lines and hackle area shown.)

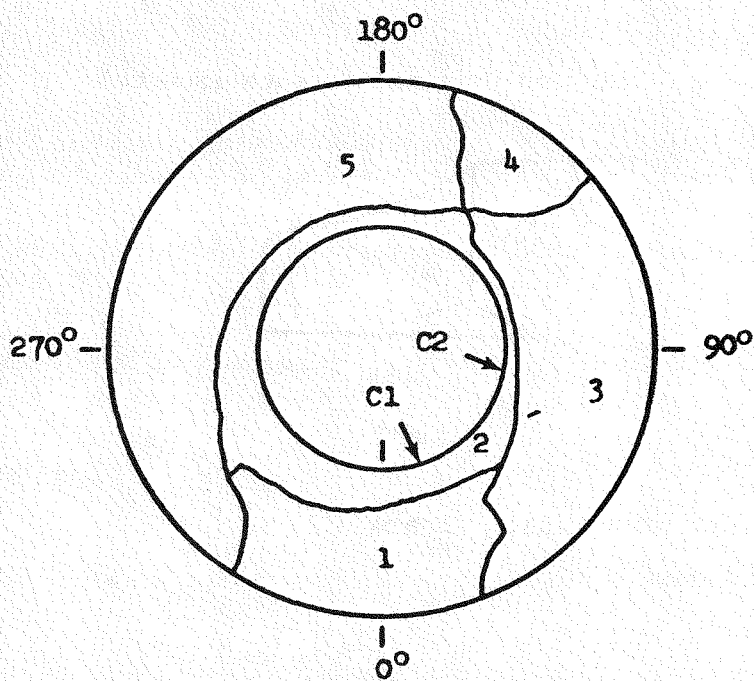


B. Schematic

Figure 4. Photograph and Schematic, Crack C2, Insulator A



A. Photograph. (The molybdenum has been etched away.)



B. Schematic Showing Origin of Cracks C1 and C2. (These originated near the bottom surface.)

Figure 5. Photograph and Schematic Bottom View, Insulator B

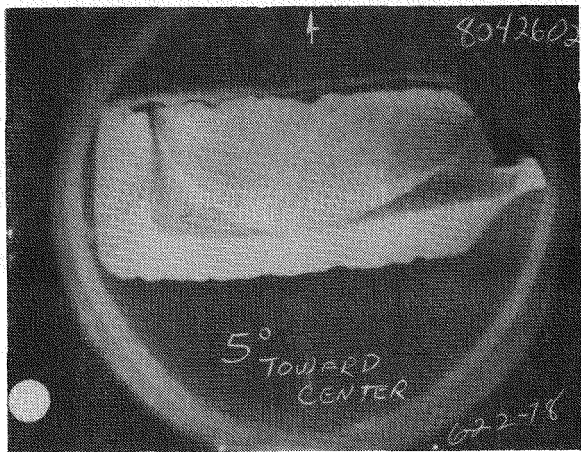


Figure 6. Photograph of Crack No. 1. Insulator B. (Photograph taken at 5° from origin [see Figure 4-B]. The crack originated at the insulator-inner sleeve interface near the bottom [inside tube] surface.)

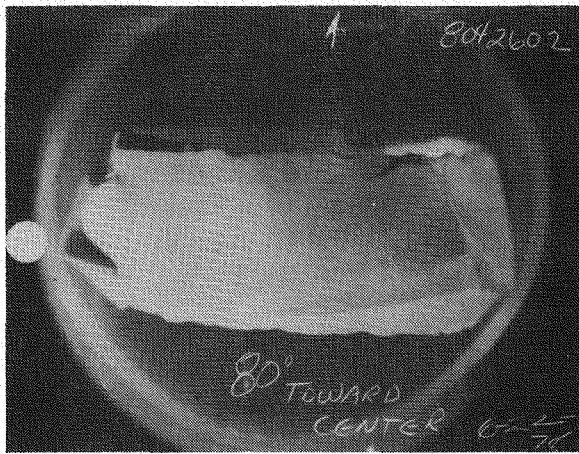


Figure 7. Photograph of Crack No. 2. Insulator B. (Photograph taken at 80° from origin [see Figure 4-B]. This crack originated at the insulator-inner sleeve interface near the bottom [inside tube] surface.)

Insulator C

Apparently during the tube removal processing this insulator had cracked but individual pieces had not separated. A photograph of the insulator in which Zyglo was used to detect cracks is shown in Figure 8. Photographs of the inside surface of the insulator after separation of the cracked pieces are shown in Figure 9. Three pieces were available for inspection.

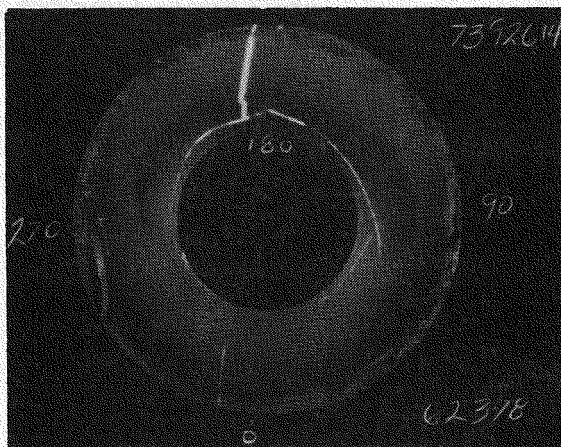
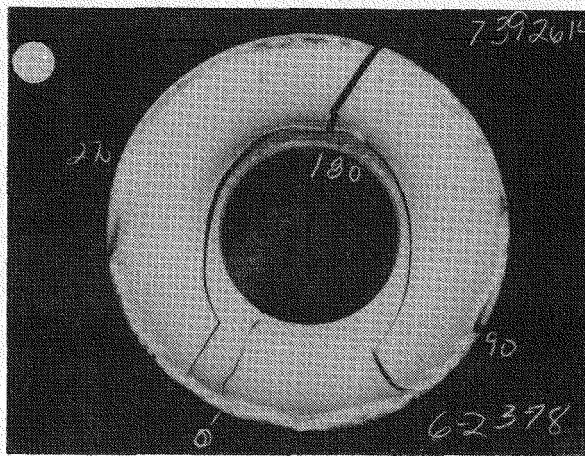


Figure 8. Photograph of Bottom Surface, Insulator C. (Photograph taken under ultraviolet light showing adsorption of Zyglo in the cracked portion.)

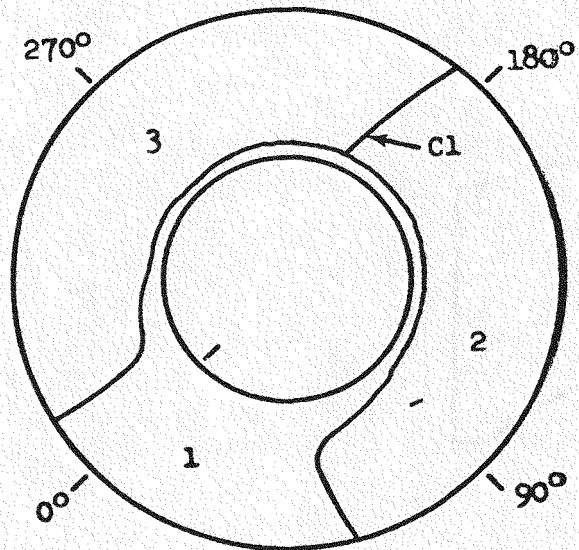
The initiation point was found to be within the insulator approximately 0.050 in. from the inner sleeve and midway between the top and bottom surfaces (see Figure 10).

INTERFACE VOID ANALYSIS

After all test specimens had been removed from the parts of the insulator, the remaining molybdenum-insulator interfaces were examined using the resin replica method.²

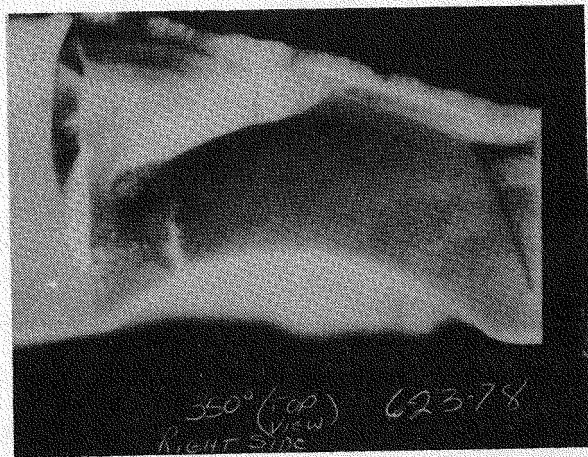


A. Photograph. (The molybdenum has been etched away.)

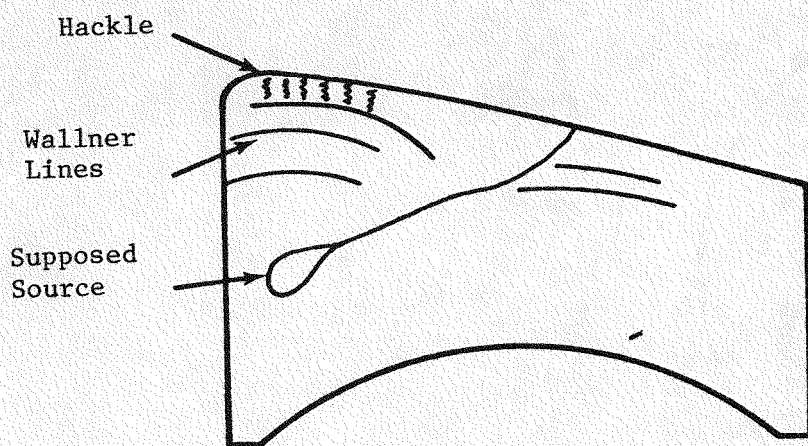


B. Schematic. (The crack originated at C1 about midway between the upper and lower surfaces of the insulator.)

Figure 9. Photograph and Schematic, Bottom View, Insulator C



A. Photograph



B. Schematic

Figure 10. Photograph and Schematic,
Fracture in Insulator C

Replicas of the inner sleeves of these units showed extensive defects (voids) at the interface of all three parts. Deep machine grooves (Figure 11) were observed on the replicas of Insulator A and Insulator C. Defects at these interfaces were spherical in shape for the most part and smooth with an exception shown in Figure 12--a smooth but irregular shaped defect from Insulator A. A substructure surface pattern appears on this defect. Flaws at the interface of Insulator B were also smooth but many were nonspherical (see Figures 13 and 14). All of the glass-ceramic residue was not removed from this replica. None of the flaws observed were as large in diameter as 0.020 in., which is the approximate size detectable by ultrasonic scanning. The maximum defect size appeared to be no larger than 0.010 in. However, clusters of voids of this size certainly should be detectable with ultrasonic examination. This examination was made of approximately 20 percent of the entire seal area. Thus, defects larger in diameter than 0.010 in. could be present at these interfaces.

The outer interfaces on all three units showed smooth, spherical voids with a maximum size of about 0.002 in. Thus, these flaws were much smaller than those at the inner sleeve interface. Interesting flaws that appeared to be due to creases or scratches in the molybdenum were evident on Insulator B (Figures 15 and 16) and Insulator B (Figure 17). In Figure 15, void defects are lodged within a "scratch." Smaller scratch marks due to polishing (typical of those seen in Figures 15, 16 and 17) were seen on the interface replicas of all three units. A cluster of voids was observed at the interface of Insulator B (see Figure 18 at 100X and Figure 19 at 1000X). These smooth, spherical nodules are typical of the defects observed at all three interfaces. As mentioned in previous reports, the cause of these defects is not precisely known but evolution of gas from the molybdenum is strongly suspected to be the source.

PERCENT SODIUM

An analysis for sodium oxide was performed using atomic adsorption spectroscopy. The weight percent of sodium oxide in the three samples was 4.57 percent, 4.54 percent and 4.51 percent for Insulators A, B and C, respectively. This is in close agreement with the theoretical amount of 4.6 wt% and well within the range of sodium oxide measured previously on this composition of glass-ceramic.

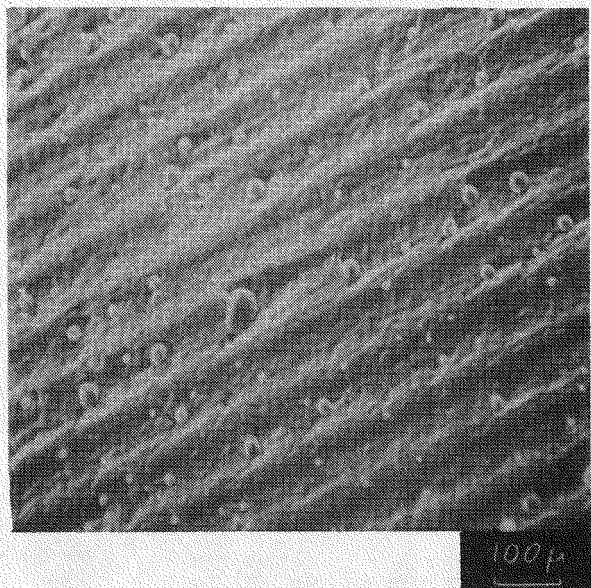


Figure 11. SEM Photograph, Insulator-Sleeve Interface.
Insulator A. 100X Magnification. (A similar condition was present on Insulator C.)

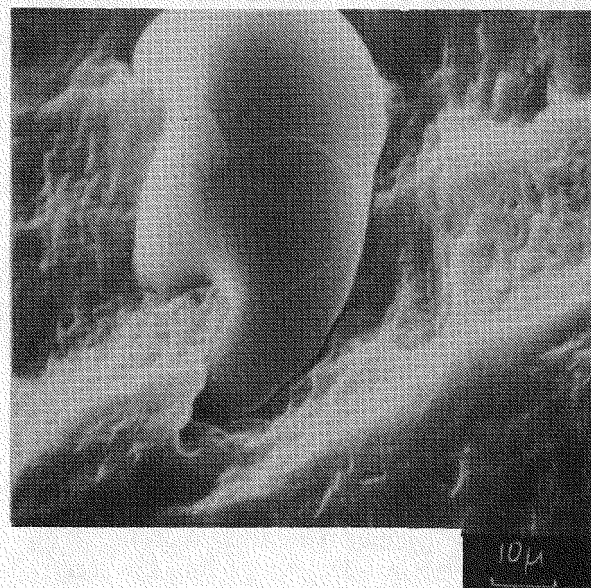


Figure 12. SEM Photograph, Insulator-Sleeve Interface.
Insulator A. 1000X Magnification. (Not surface structure on defect.)

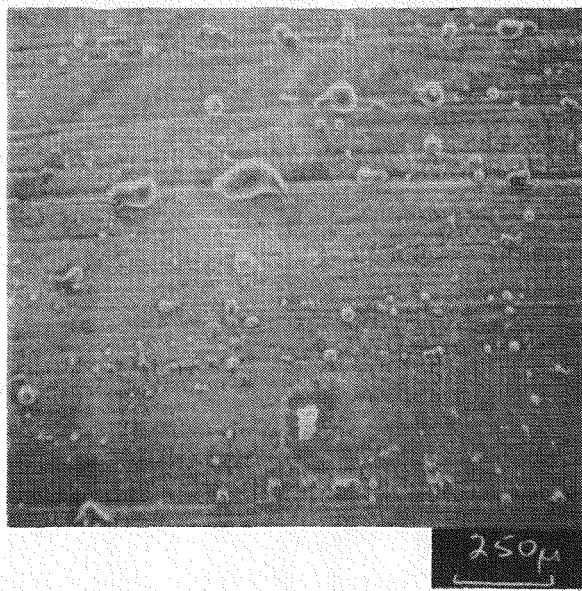


Figure 13. SEM Photograph,
Insulator-Sleeve
Interface.
Insulator B.
60X Magnification.

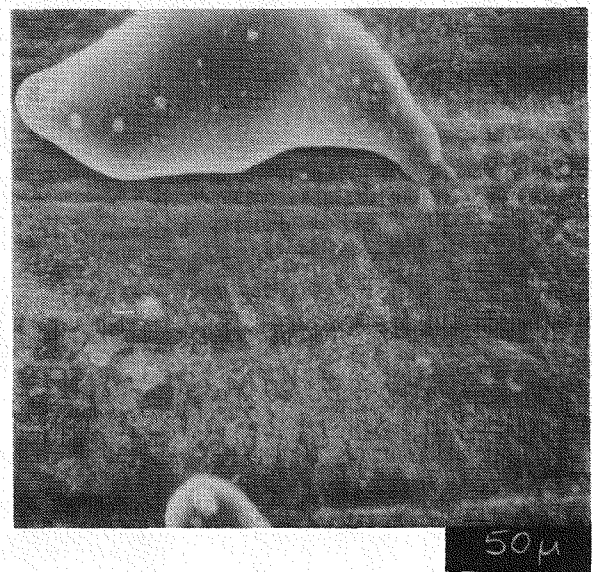
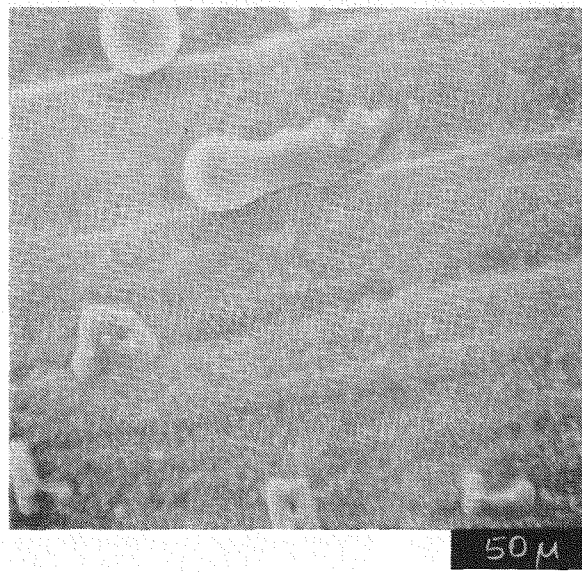


Figure 14. SEM Photographs, Insulator-Sleeve Interface.
Insulator B. 300X Magnification.

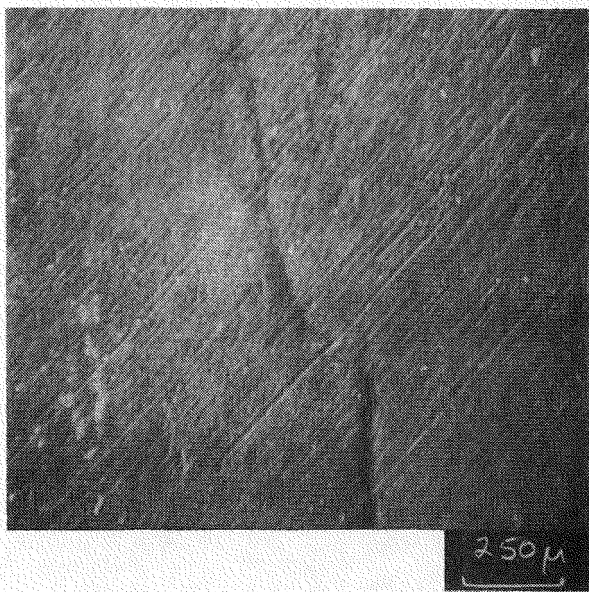


Figure 15. SEM Photograph
Showing Large
Scratch and
Smaller Polishing
Scratches.
Insulator B.
60X Magnification.



Figure 16. SEM Photograph
Showing Scratch
and Voids Lodged
in Scratches.
Insulator B.
300X Magnification.

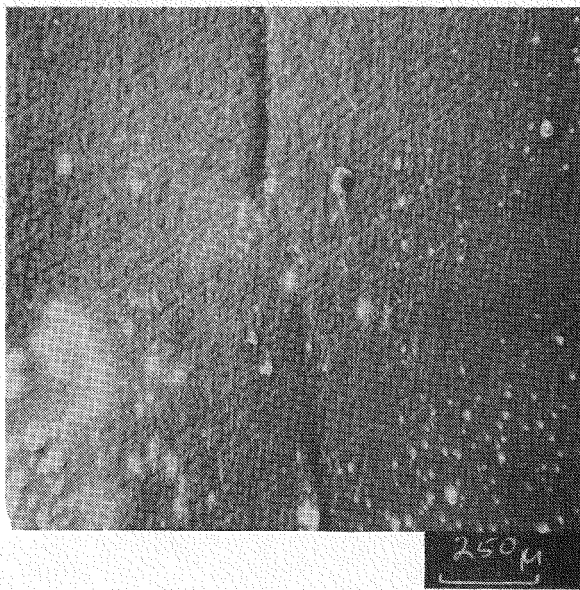


Figure 17. SEM Photograph
Showing Scratches.
Insulator A.
60X Magnification.

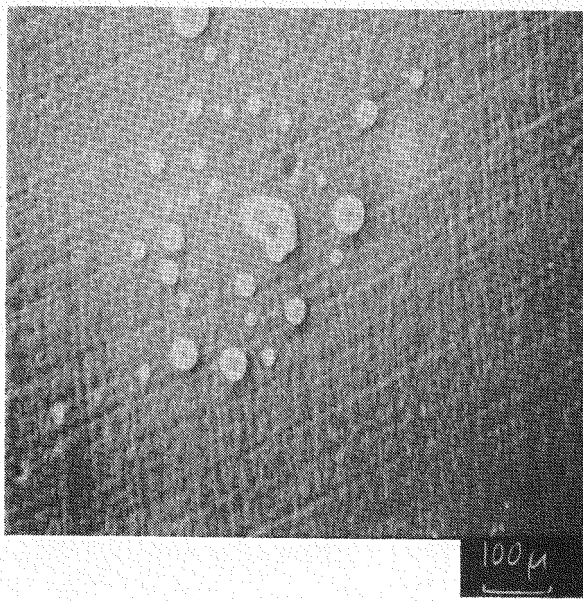


Figure 18. SEM Photograph
Showing Cluster of
Voids. Insulator A.
100X Magnification.

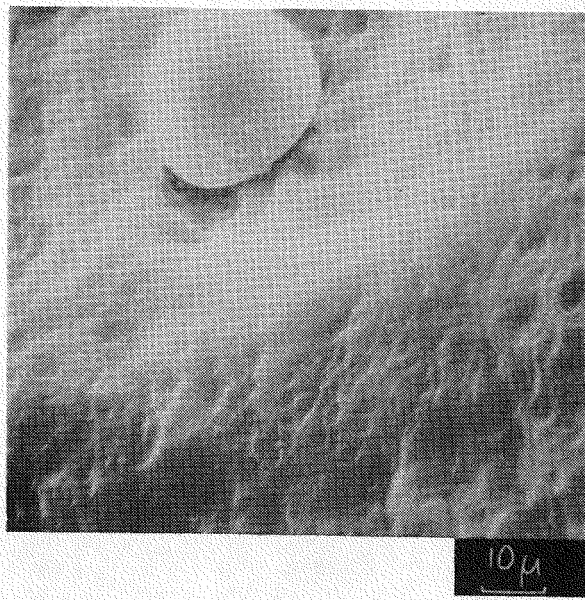


Figure 19. SEM Photograph
Magnified View
of Cluster Shown
in Figure 18.
Insulator A.
1000X Magnification.

CHEMICAL ELEMENT COMPARISON BY X-RAY EMISSION SPECTROSCOPY

Gross differences in chemical elements having an atomic number of 13 (aluminum) or above can be determined using X-ray emission spectroscopy. Due to the fact that standards were never developed for this inspection technique, the analysis is not quantitative. However, by comparing the relative count it is possible to determine major differences. For this study, a 1/4-in. square area was polished to 16 microinches and examined for Si, Al, Zn, Ba and P by comparing the X-ray counts for a 100-s exposure in each sample. The results (shown in Figure 20) show no substantial differences in chemical content of the three samples submitted.

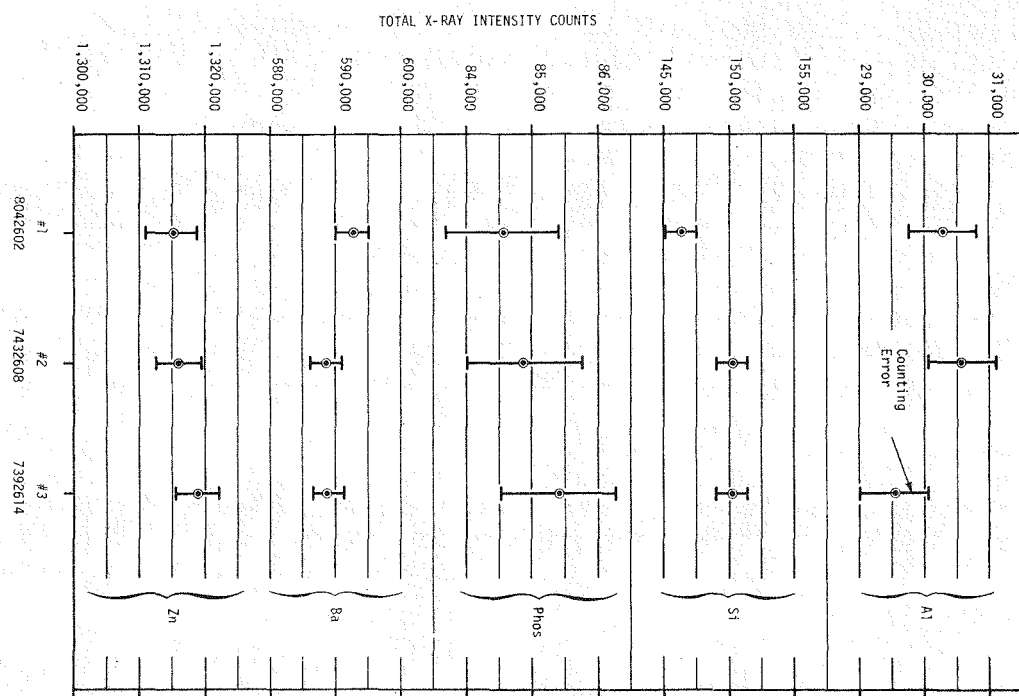


Figure 20. Graphical Comparison of Chemical Differences Detected in Insulators Using X-ray Emission

COEFFICIENT OF EXPANSION

A coefficient of expansion sample measuring $0.1 \times 0.1 \times 1$ inch was removed from the largest piece of insulator available. The expansion between room temperature and 600°C was measured using a quartz push rod dilatometer. The coefficient of

expansion for these samples was $51.9 \times 10^{-7}/^{\circ}\text{C}$, $53.0 \times 10^{-7}/^{\circ}\text{C}$ and $53.9 \times 10^{-7}/^{\circ}\text{C}$ for Insulators A, B and C, respectively. These coefficients are within the specification limits and should not present a residual stress state that is crack prone.

It was possible to trace the insulator back to the glass lot number on only Insulator B. For this insulator, the glass lot coefficient of expansion was $51.6 \times 10^{-7}/^{\circ}\text{C}$ when originally tested. The difference between the value determined in this test and that determined originally is within the two percent accuracy of this test.

DIFFERENTIAL THERMAL ANALYSIS

A differential thermal analysis thermogram was made on cubes (0.125 in. edge) from each of the three insulators. This analysis, using the second highest sensitive scale, showed a minor amount of activity in the crystal growth region. With the high sensitivity scale, there was considerable noise that may have been interpreted as annealing or ceraming activity. The rerun thermogram of the three samples showed a definite decrease in activity at 750 to 850°C . Figure 21 is a copy of the thermogram for Insulator A and is typical of all three units. The precise cause of this additional thermal activity or effect on the insulator is not known. The activity may be associated with coarsening of the crystalline phase of the glass-ceramic which has been evident in the past.

MICROSTRUCTURE

A SEM microstructural examination was made on samples prepared by ceramographic polishing followed by etching in hydrofluoric acid fumes for ten seconds. The microscope of insulators from all units was typical of MS11 glass-ceramic.

RESULTS

Examinations show that no substantial differences exist between the insulators, molybdenum condition or basic interface characteristics of these units. Examination of the surface of Insulator B indicated that the fracture initiated at the inner sleeve-insulator interface in an area of high void density. Voids at the inner sleeve-insulator interface were also present on Insulator A but none were detected at the crack origin. The crack in Insulator B may have been initiated by stresses imposed during shock testing, whereas on Insulator A, cracks on the inside of the tube on the insulator were not evident until the tube was removed. Thus, it may be that shock testing overstresses the tube near the top where the cracks on

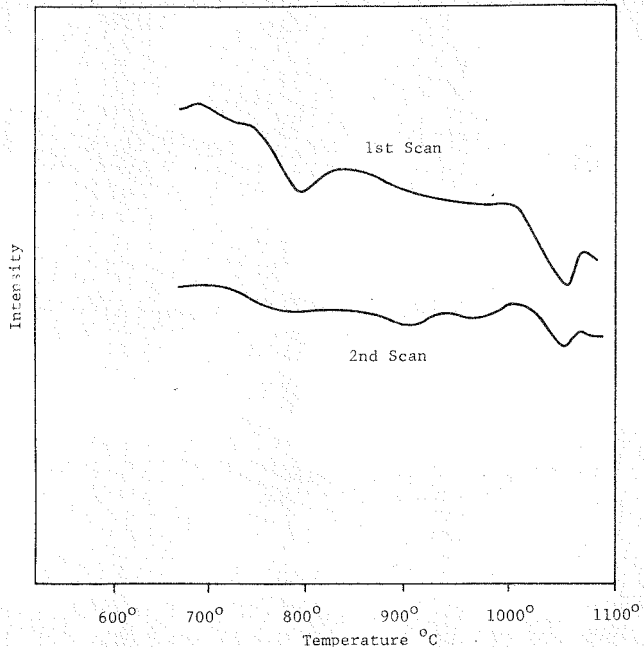


Figure 21. Comparison of Differential Thermal Analysis Thermograms. Insulator A. (The second scan is a repeat of the sample scanned initially. These are typical of the results on all three insulators. The decrease in activity at 800°C during the second scan is of interest.)

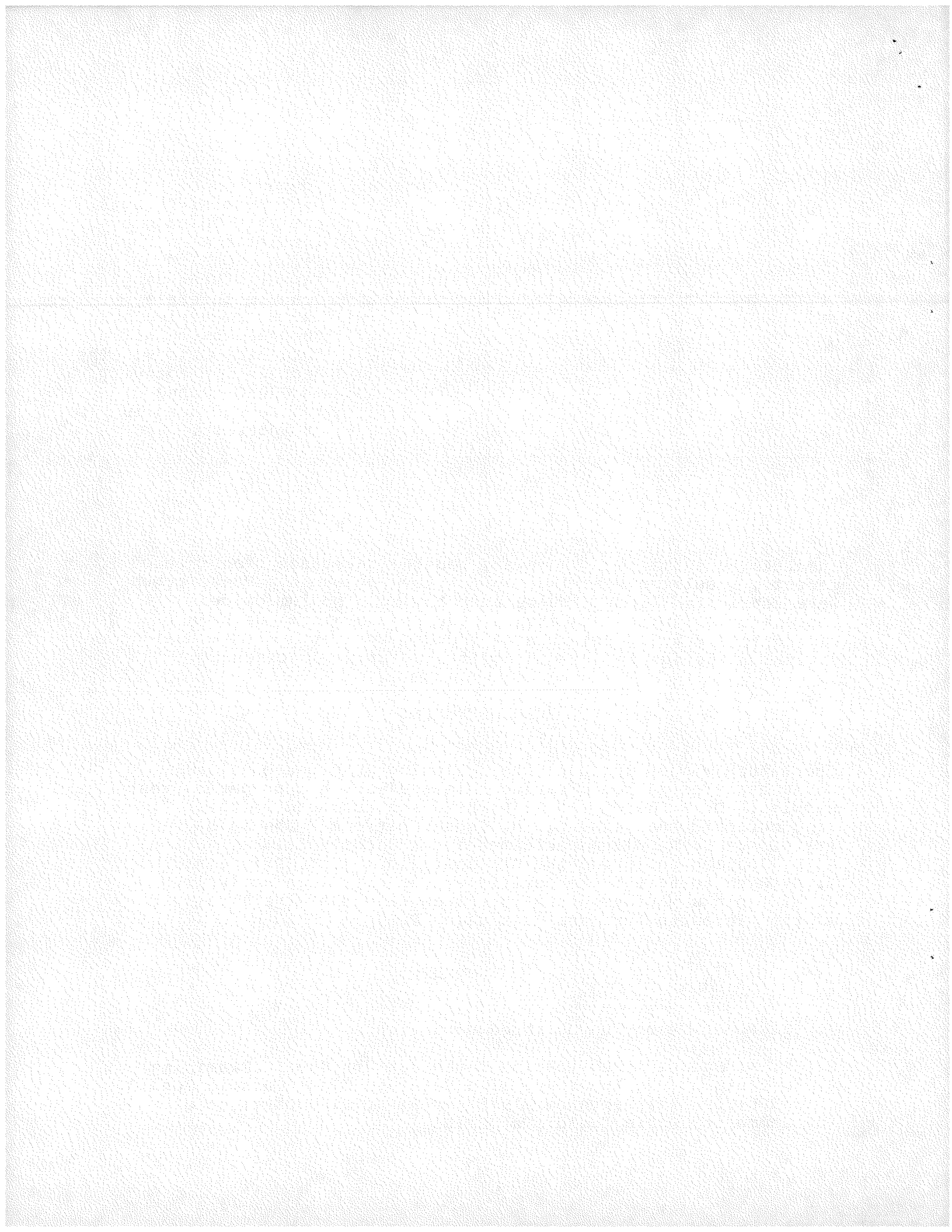
Insulator B initiated. However, had the interface been free of defects, insulator cracking may not have occurred. These tubes were fabricated from glass-ceramic having a sodium oxide content of 4.6 wt%. Since then, the Na₂O content has been raised to 4.8 wt%. This change reduced the level of residual stress in the insulator, making it less prone to cracking.

ACKNOWLEDGMENTS

The author wishes to thank the following GEND personnel. J. Davis assisted in coordinating this analysis and preparing test samples. D. B. Hardy and B. P. J. Cason assisted in the fractographic analysis. J. M. Carter performed the Na₂O analysis. E. N. Kling performed the XRE analysis. L. L. Johnson performed the DTA analysis. J. T. Prince and J. F. Ryan performed the coefficient of expansion analysis. J. E. Spinks performed the interface defect analysis as well as the microstructure analysis using SEM.

REFERENCES

1. B. P. J. Cason, unpublished data
2. R. K. Spears, "Replication Technique for Use in Examining Defects in the Interface of a Metal-to-Glass Ceramic Bond," GEPP-TIS-391, September 1978, NTIS, U. S. Department of Commerce, Springfield, Va. 22161



DISTRIBUTION

DOE

P. M. Ramey, PAO
TIC, Oak Ridge (27)

GE

Technical Information Exchange
Schenectady (5)

GEND

J. T. Davis
A. N. Kenly
R. K. Spears
S. N. Suciu

Technical Data Library (10)
Technical Report Writer (1 + Reproduction Masters)

Sandia National Laboratories, Albuquerque

B. E. Barnaby 2354
R. J. Eagan 5845